Journal of Hazardous Materials 192 (2011) 307–313

Contents lists available at ScienceDirect

Journal of Hazardous Materials

journal homepage: www.elsevier.com/locate/jhazmat

A new model of repulsive force in eddy current separation for recovering waste toner cartridges

Jujun Ruan, Zhenming Xu*

School of Environmental Science and Engineering, Shanghai Jiao Tong University, 800 Dongchuan Road, Shanghai 200240, People's Republic of China

ARTICLE INFO

Article history:
Received 15 January 2011
Received in revised form 18 April 2011
Accepted 9 May 2011
Available online 14 May 2011

Keywords:
Waste toner cartridges
Model of repulsive force
Detachment angle

ABSTRACT

Eddy current separation (ECS) is an efficient method for separating aluminum from plastic in crushed waste toner cartridge (TCs). However, in China, ECS quality of aluminum from plastic is rather low in production practice. Repeating separation even manual sorting is required in the production. Improving separation quality of aluminum has been the pressing problem in the recovery of waste TCs. Furthermore, improving ECS quality can reduce the secondary-pollution (furan and dioxin) brought by plastic in later smelting process for the purification of recovered aluminum. Thus, a new model of repulsive force containing impact factors (machine: B_r, k, R, S_m, B_m; material: S_p, V, γ; and operation: ω_m, v, δ) of the separation process was constructed for guiding the ECS process of waste TCs recovering in this paper. For testing whether the model of repulsive force was suitable to guide the ECS, calculation and experiment of detachment angle of aluminum flake were studied. The calculation results of the detachment angles were agreed with the testing experiment. It indicates that the model is suitable for guiding the ECS of waste TCs recovering.

1. Introduction

Quantities of electronic waste (e-waste) have been generated along with the technological innovation and the social development. People have attached much importance to the spawn of e-waste because of the contained resource and the potential environmental pollution [1–6]. Lager numbers of waste toner cartridges (TCs) have been generated as the result of the renovation of printers and duplicators. Waste TC contains abundant plastic, aluminum, steel, permanent magnet, and residual toxic toner. Recovery of waste TC will bring renewable resources coexisting with environmental risk. An environment-friendly technology of waste TCs recovering has been developed [7]. It was comprised of shearing process, toner collecting, magnetic separation, and eddy current separation (ECS). ECS was used to separate aluminum from the plastic of crushed waste TC. ECS has been an effective separation technology in resource recycling industries such as recycling light metals from end-of-life vehicles [8–11]. It is also a good recovery technology for e-waste such as discarded PC, end-of-life household appliances, etc. [12,13]. However, in China, ECS quality of aluminum from plastic is rather low in the production practice of waste TCs recovering. Repeating separation even manual sorting is required in the production. Improving separation quality of aluminum has been the pressing problem in the recovery of waste TCs. Furthermore, the final treatment of the aluminum recovered from waste TC is smelting for purification. Improving separation quality can reduce the secondary-pollution (dioxin and furan) brought by plastic in later smelting process for the purification of recovered aluminum. These problems cause us to research the separation mechanism of ECS. Repulsive force generated between nonferrous (aluminum, copper, etc.) and eddy current separator is the major cause of separating nonferrous from nonmetals.

Very valuable information has been reported about the repulsive force by the researchers such as the groups of P. Rem, P. Bevilacqua, E. Forssberg, Z. Schlett and M. lungu. Rem and his group presented a model of repulsive forces for the motion of particle in ECS for optimizing separator design and operation. The model not only describes the magnetic moments of the particle but also regards the effects of particle size, shape, and conductivity on the particle trajectory [14]. Later, Maraspin and Bevilacqua improved the model of the repulsive force and simulated the motion of particle in ECS by computer software. They found the primary impact factors were size, conductivity, and initial orientation of particle [15]. Zhang and Forssberg reformed the model of the repulsive force for processing small particles by ECS, and found strengthening the magnetic field intensity and increasing the maximum drum speed could enhance the performance of eddy current separators [16]. Z. Schlett and M. Lungu presented the model of repulsive force in a new device of ECS for separating aluminum from a mixture of millimetric Al–Cu wires [17].

* Corresponding author. Tel.: +86 21 54747495; fax: +86 21 54747495.
E-mail address: zmxu@sjtu.edu.cn (Z. Xu).

0304-3894/$ – see front matter © 2011 Elsevier B.V. All rights reserved.
doi:10.1016/j.jhazmat.2011.05.025

Nomenclature

b_n	Fourier coefficient
B_m	magnetic flux density of the magnetic drum surface (T)
B_p	induced magnetic flux density in the particle (T)
B_r	magnetic flux density of the field (T)
F_r	repulsive force between the particle and the magnet (N)
g	acceleration of gravity force (m/s^2)
G	gravity force of the aluminum flake (N)
J	induced eddy current in flakes (A)
k	number of pairs of the magnets placed in the magnetic drum
l	height of the rectangle/triangle flake (m)
L	circumference of the triangle flake (m)
r	radius distance between the particle and the center of magnetic drum (m)
r'	radial distance between the particle and the inducing magnet (m)
R	radius of the magnetic drum (m)
S_m	per magnet side area which facing the flake (m^3)
S_p	maximal cross area of the flake in horizontal (m^2)
t	time cost for the magnetic field rotation (s)
T	thickness of the flake (m)
v	feeding speed of the flake (m/s)
v'	relative linear velocity between the flake and magnetic drum (m/s)
V	volume of the rectangle/triangle flake (m^3)
w	width of the rectangle/triangle flake (m)
Ω	resistance of circular/rectangle/triangle coil
α_0	angle of the coordinate in the cylindrical coordinate system
γ	conductivity of the flake (S/m)
δ	oriental factor of the flake in eddy current separation
ε_i	induced emf in the circular/rectangle/triangle coil (V)
μ_r	relative magnetic permeability of iron (H/m)
μ_0	magnetic permeability of vacuum (H/m)
ω_m	rotation velocity of the magnetic drum (rad/s)
Φ_p	induced magnetic flux in the particle (Wb)
Φ_m	magnetic flux of the permanent magnet (Wb)
$\Delta\Phi$	variation of magnetic flux in the particle (Wb/s)

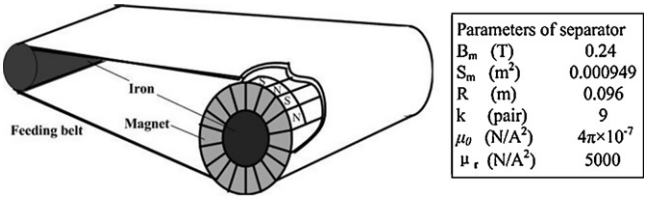

Fig. 2. The structure of the eddy current separator.

During the process of using these model to guide the ECS of waste TCs recovering, some unreported factors (such as area of per magnet that facing the particle and maximal cross area of the particle in horizontal), which affected the separation quality, were discovered. Based on the simulation of magnetic field and the analysis of induced eddy current in aluminum flake, a new model of repulsive force containing the unreported factors was constructed in order to investigate the impact factors of ECS in this paper. For testing whether the model of repulsive force is suitable to guide the ECS, calculation and experiment of detachment angle of aluminum flake from the conveyor belt in ECS are researched in this paper.

2. Materials and method

2.1. Materials

Materials employed to this study were collected from crushed waste TC. Aluminum components of waste TC were crushed into flakes by shearing process. The maximal and minimal aluminum flakes, with the representative shape of circle, rectangle, and triangle, were selected for the construction of the model of repulsive force and the testing experiment. They were marked as C1, C2, R1, R2, T1, and T2 (Fig. 1). Physical properties of the selected aluminum flakes are given in Fig. 1. Eddy current separator employed to this study was horizontal drum eddy current separator (Fig. 2). Magnetic drum is comprised of iron core covered by nine pairs of NdFeB magnets, placed with N–S–N orientation respectively. Physical properties of the separator are presented in Fig. 2.

2.2. Calculation process of the repulsive force

In ECS process of recovering aluminum from plastic of crushed waste TCs, eddy current will be induced in aluminum flake as getting into the magnetic field that provided by eddy current separator. Immediately, new magnetic flux, with the opposite direction of the inducing magnetic flux from the magnet, will be generated in alu-

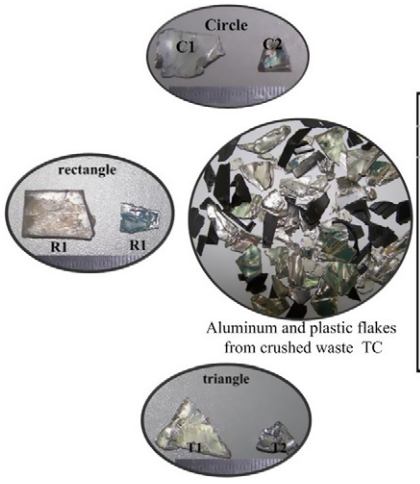

Physical property of aluminum used in the calculation

		C1	C2	R1	R2	T1	T2
A1	size (L×W×T, mm)	15×15×2	5×5×2	15×5×2	10×5×2	15×5×2	10×5×2
	shape	circle	circle	rectangle	rectangle	triangle	triangle
	γ (S/m)	3.5×10^7					
	S_p (cm^2)	1.77	0.2	0.75	0.5	0.375	0.25
	V (cm^3)	0.354	0.04	0.15	0.1	0.075	0.05
	G (10^{-3},N)	9.70	1.40	4.12	2.74	2.06	1.37

Fig. 1. Selected aluminum flakes employed to the construction of repulsive force model and testing experiment.

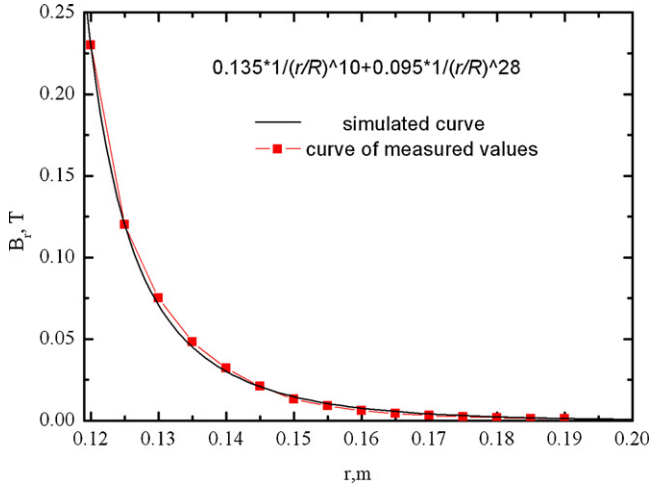

Fig. 3. Curves of magnetic flux density by simulating and measuring the applied magnetic field.

minum flake. Aluminum flake can be considered as a new induced magnetic pole. Then, repulsive force (F_r) will be produced between the induced magnetic pole and the magnet of the separator. This repulsive force causes the aluminum flake separated from plastic. The derivation of the model of repulsive force was based on considering the aluminum flake as an induced magnetic pole.

2.2.1. Simulation of magnetic flux density and distribution of the applied magnetic field

Alternating magnetic field will be produced around the magnetic drum by the rotation of eddy current separator. The magnetic flux density of the field yields to the following formulas in a cylindrical coordinate system (r, α, z) relative to the drum axis [14]:

$$B_r = \sum_{n=0}^{\infty} b_n (r/R)^{-(2n+1)k-1} \sin(2n+1)k(\alpha - \omega_m t) \quad (1)$$

$$B_\alpha = \sum_{n=0}^{\infty} b_n (r/R)^{-(2n+1)k-1} \cos(2n+1)k(\alpha - \omega_m t) \quad (2)$$

$$B_z = 0 \quad (3)$$

The values of parameter R and k of the eddy current separator are 0.096 m and 9 pair. Since the big gaps of size and rotation speed between the particle and the magnetic separator in ECS, alternating magnetic flux can be supposed as crossing over the aluminum flake vertically when the flake gets close to magnet. Thus, the value of $(\alpha - \omega_m t)$ can be supposed as 90°. Fourier coefficient (b_n) can be obtained by measuring the magnetic flux density and the corresponding value of radial distance (r). The values of the Fourier coefficients b_0 and b_1 of the applied alternating magnetic field are 0.135 and 0.095 respectively. Thus, Eqs. (1)–(3) can be simplified into Eq. (4) that presented the magnetic flux density of the applied alternating field:

$$B_r = 0.135(r/R)^{-10} + 0.095 \times (r/R)^{-28} \quad (4)$$

The curve of the magnetic flux density of the applied alternating field was plotted and given in Fig. 3. Density gradient of the magnetic flux was also measured by teslameter and the result was given as the red curve in Fig. 3. It can be seen that the simulation result of the magnetic flux density is agreed with the measure. So formulas (4) are suitable for calculating the magnetic flux density of the applied alternating field. Furthermore, the distribution of the magnetic flux of the applied magnetic field was simulated by the multi-physics coupling analysis software called Comsol. Magnetic flux distribution was investigated in two space dimensions and instantaneous. Simulation imagination is given in Fig. 4 and the result indicates that the alternating magnetic field is a periodic and finite field. Magnetic flux density decreases as the distance increasing from magnet surface. Since the weak magnetic permeability of air, the gradient of magnetic flux density is very great and high-intensity magnetic flux distributes in a small area near to magnet surface. The range of magnetic flux density is from 7.2×10^{-11} to 0.429 T.

2.2.2. Calculation of the eddy current in aluminum flake

As aluminum flake moving near to the rotating magnetic drum in ECS, the relative linear velocity between the flake and magnet can be expressed as:

$$v' = v - \omega_m R$$

The applied alternating magnetic flux is supposed to cross the flake vertically since the big gaps of size and speed between the flake and the magnetic drum. Therefore, the suffered variation of magnetic flux of the flake can be given as:

$$\Delta\Phi = \iint_s B_r dS_p$$

Due to the change of magnetic flux, eddy current will be induced in aluminum flake. According to current skin effect, the current forms yield to the shape of the maximal cross area of the particle. Eddy current forms of the aluminum flakes are presented in Fig. 5b.

2.2.2.1. The calculation of eddy current induced in circle aluminum flake. The induced eddy current in circle aluminum flake is calculated in the following assumption. The radius of the circle aluminum flake is presented as R_p. Circular coil (radius τ; thickness h) is supposed to exist in the circle flake (Fig. 5b). Then the suffered variation of magnetic flux of the circular coil can be expressed in:

$$\Delta\Phi = B_r \pi \tau^2$$

According to Faraday induction law, the value of the electromotive force induced in circular coil is:

$$\varepsilon_i = -\frac{B_r \pi \tau^2 k(\omega_m R - v)}{\pi R}$$

Resistance of the circular coil can be presented in the following equation:

$$d\Omega = \frac{1}{\gamma} \frac{2\pi\tau}{T d\tau}$$

Then, eddy current density in the circular coil is:

$$dJ = \frac{B_r k(\omega_m R - v)\gamma T \tau d\tau}{2\pi R}$$

Then the induced eddy current (J^C) in circle aluminum flake can be calculated by the integration of dJ:

$$J^C = \int dJ = \frac{B_r k(\omega_m R - v)\gamma T}{2\pi R} \int_0^{R_p} r dr = \frac{B_r k(\omega_m R - v)\gamma T}{4\pi R} R_p^2$$

2.2.2.2. The calculation of eddy current induced in the rectangle aluminum flake. The induced eddy current in circle aluminum flake is calculated in the following assumption. The side length and width of the rectangle aluminum flake are signed as L and W respectively (Fig. 5b). Concentric rectangle coil (long $(w/W)L$; wide w; thickness T) is supposed to exist in rectangle flake. Then the variation of magnetic flux crossing the rectangle coil is expressed in:

$$\Delta\Phi = B_r \frac{w^2}{W} L$$

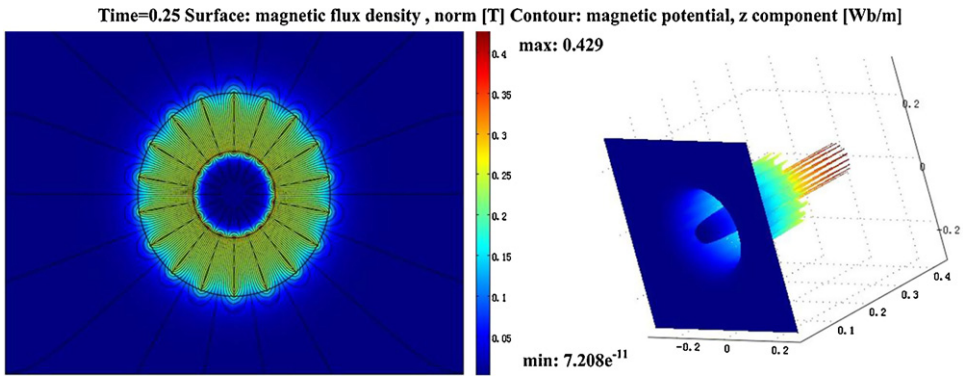

Fig. 4. The 2D and 3D surface diagram of simulation distribution of magnetic flux density with COMSOL 3.4.

According to Faraday induction law, the value of the electromotive force induced in rectangle coil is:

$$\varepsilon_i = -\frac{B_r(w^2/W)Lk(\omega_m R - v)}{\pi R}$$

Resistance of the rectangle coil can be expressed as:

$$d\Omega = \frac{1}{\gamma}\frac{2w((L/W)+1)}{Td(w/2)}$$

Then, the value of the induced eddy current in rectangle coil is:

$$dJ = \frac{B_r k\gamma(\omega_m R - v)TLwd(w/2)}{2\pi RW((L/W)+1)}$$

Then the induced eddy current (J^R) in rectangle aluminum flake can be calculated by the integration of dJ:

$$J^R = \int dJ = \frac{B_r k\gamma(\omega_m R - v)TL}{2\pi RW((L/W)+1)}\int_0^{W/2} wd\frac{w}{2} = \frac{B_r k\gamma(\omega_m R - v)TLW^2}{8\pi RW((L/W)+1)}$$

2.2.2.3. The calculation of eddy current induced in the triangle aluminum flake. The induced eddy current in circle aluminum flake is calculated in the following assumption. The bottom margin, height, circumference, and thickness of the triangle aluminum flake are signed as W, L, C, and T respectively. Concentric triangle coil with bottom margin $(l/L)W$, height l, circumference $(l/L)C$, and thickness T is supposed to exist in the triangle aluminum flake (Fig. 5b).

Then the variation of magnetic flux crossing the triangle coil can be expressed as:

$$\Delta\Phi = B_r\frac{l^2 W}{2L}$$

According to Faraday induction law, the value of the induced electromotive force in triangle coil is:

$$\varepsilon_i = -\frac{B_r l^2 Wk(\omega_m R - v)}{2L\pi R}$$

Resistance of the triangle coil is presented in the following equation:

$$d\Omega = \frac{1}{\gamma}\frac{lC}{LTd(l/2)}$$

Then the value of induced eddy current in triangle coil is:

$$dJ = \frac{B_r\gamma k(\omega_m R - v)WTld(l/2)}{2\pi RC}$$

In finals, the induced eddy current (J^T) in triangle aluminum flake can be calculated by the integration of dJ:

$$J^T = \int dJ = \frac{B_r\gamma k(\omega_m R - v)WT\int_0^{l/2}(l/2)d(l/2)}{\pi RC}$$

$$= \frac{B_r\gamma k(\omega_m R - v)TWL^2}{8\pi RC}$$

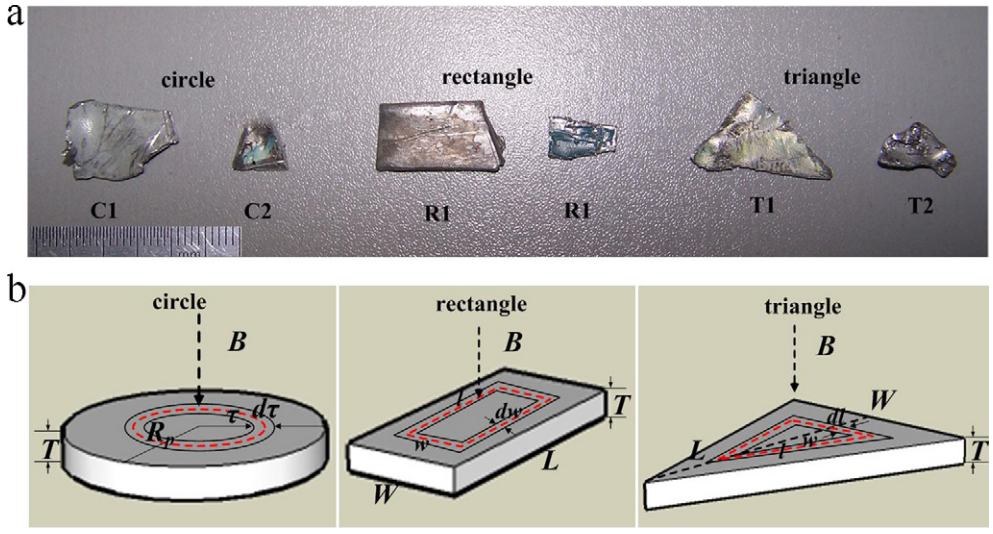

Fig. 5. The analysis of the detachment moment of aluminum flake in ECS.

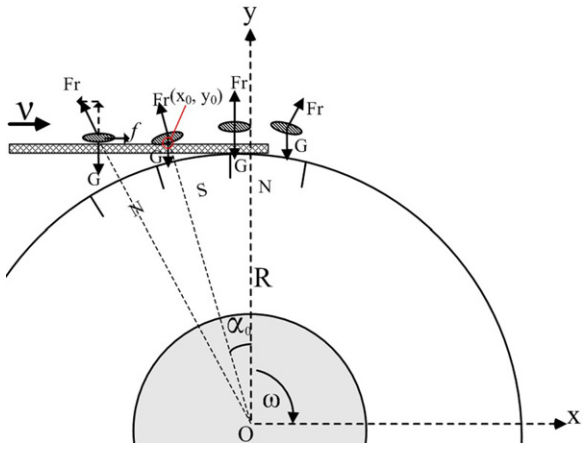

Fig. 6. The representative flakes and induced currents.

2.2.3. Calculation of the induced magnetic flux in aluminum flake

Induced magnetic fluxes of the various aluminum flakes in ECS are calculated based on the theory of Biot-Savart law. In ECS, eddy current is induced in aluminum flake as undergoing the alternating magnetic field. Immediately, new magnetic flux will be produced in the flake by the induced eddy current. The induced magnetic flux and density is nearly expressed as:

$$B_p = \mu_0 J, \quad \Phi_p = B_p S_p$$

Thus the induced magnetic fluxes of circle, rectangle, and triangle aluminum flake can be expressed as following equations respectively after defining $\delta_R = W/(2(L+W))$ and $\delta_T = L/C$.

$$\Phi^C = \frac{B_r k(\omega_m R - v)\gamma V S_p \mu_0}{4\pi^2 R} \tag{5}$$

$$\Phi^R = \frac{B_r k\gamma(\omega_m R - v) V S_p \delta_R \mu_0}{4\pi R} \tag{6}$$

$$\Phi^T = \frac{B_r \gamma k(\omega_m R - v) V S_p \delta_T \mu_0}{4\pi R} \tag{7}$$

2.2.4. Calculation of the repulsive force

New magnetic flux (Φ_p) is induced in aluminum flake by the magnetic flux (Φ_m) provided by the magnet in ECS. The aluminum flake is supposed as an induced magnetic pole. The tow magnetic poles have the backward direction. Interaction force between the induced magnetic pole and the magnet can be expressed as [18]:

$$Fr = \frac{\Phi_p \Phi_m}{4\mu_0 \pi h^2}$$

where h is the radial distance between aluminum flake and magnet. The value of this radial distance can be expressed as $h = (R/\cos\alpha_0) - R$ in ECS (see Fig. 6).

Then the repulsive force between the aluminum and magnet can be presented as:

$$Fr = \frac{\Phi_p \Phi_m}{4\mu_0 \pi R^2} \frac{1}{(\sec\alpha_0 - 1)^2} \tag{8}$$

The magnetic flux of the inducing magnet (Φ_m) is:

$$\Phi_m = B_m S_m \tag{9}$$

By inserting Eqs. (5) and (9) in Eq. (8), the repulsive force of circle flake is:

$$Fr^C = \frac{B_r k(\omega_m R - v)\gamma V S_p B_m S_m}{16\pi^3 R^3} \frac{1}{(\sec\alpha_0 - 1)^2} \tag{10}$$

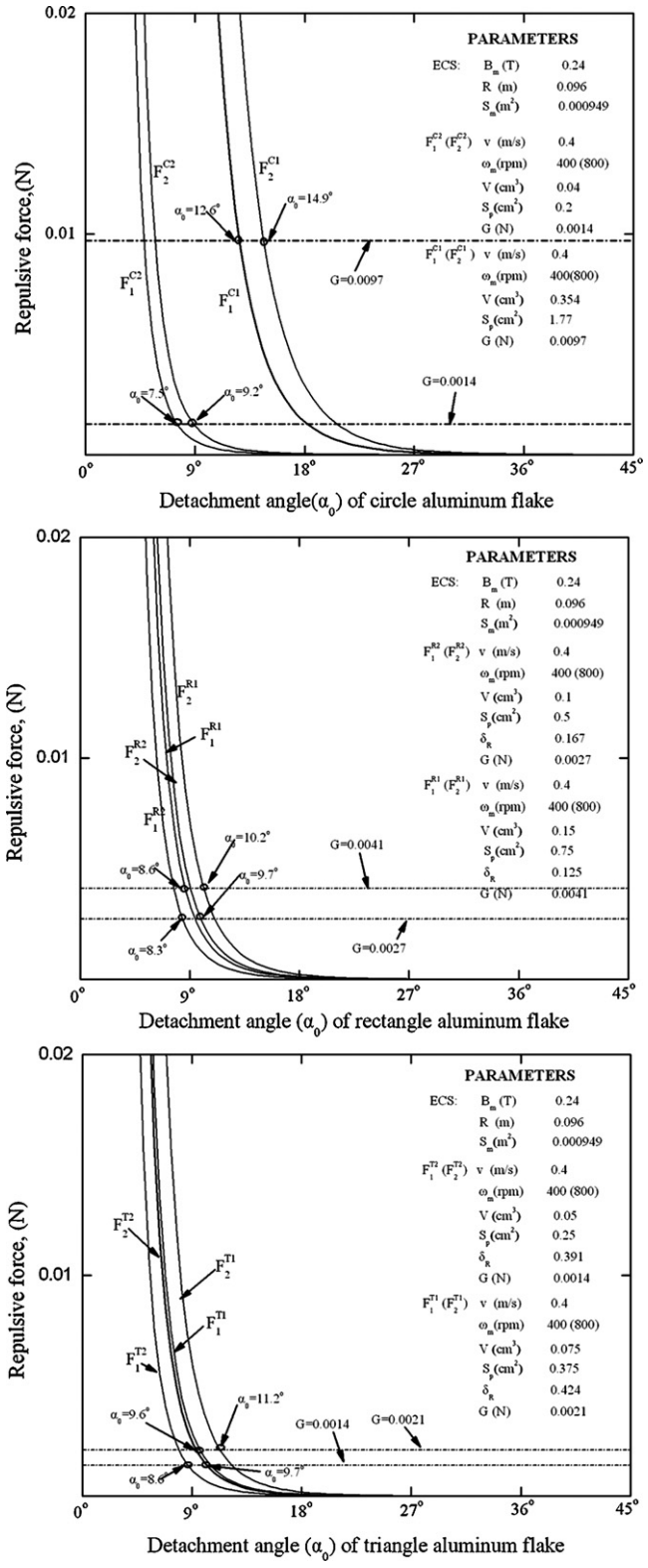

Fig. 7. The detachment angles of circle, rectangle, and triangle aluminum flakes in ECS.

By inserting Eqs. (6) and (9) in Eq. (8), the repulsive of rectangle flake can be calculated as:

$$Fr^R = \frac{B_r k\gamma(\omega_m R - v) V S_p B_m S_m \delta_R}{16\pi^2 R^3} \frac{1}{(\sec\alpha_0 - 1)^2} \tag{11}$$

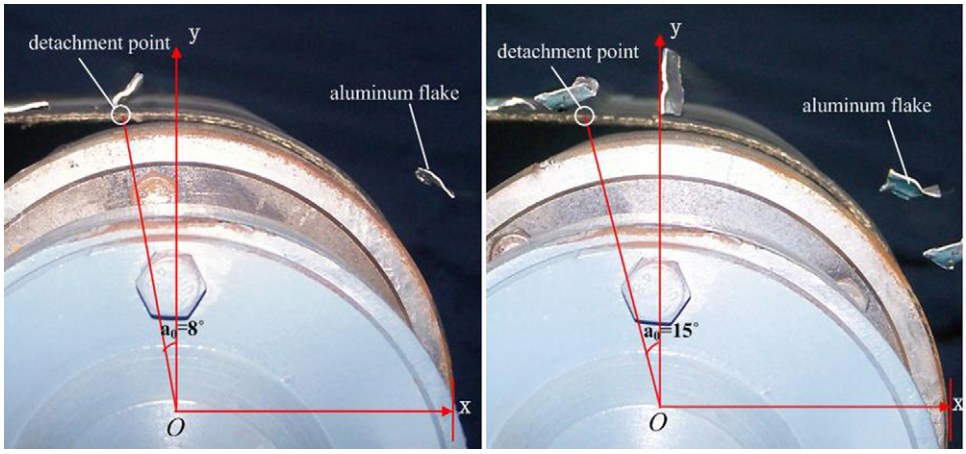

Fig. 8. The photos for investigating the detachment angle of aluminum flakes in the testing experience process.

By inserting Eqs. (7) and (9) in Eq. (8), the repulsive forces of triangle flake is calculated as:

$$Fr^T = \frac{B_r \gamma k(\omega_m R - v) V S_p B_m S_m \delta_T}{16\pi^2 R^3} \frac{1}{(\sec\alpha_0 - 1)^2} \quad (12)$$

2.3. Calculation process of detachment angle of aluminum flake in ECS

The aim of constructing the model of repulsive force generated between aluminum flake and separator is to investigate the impact factors of ECS. The ultimate purpose is to improve the ECS quality of aluminum by adjusting the impact factors that contained in the model of repulsive force. For testing whether the model of repulsive force is suitable to guide the ECS, calculation and experiment of detachment angle of aluminum flake are studied in the following content.

2.3.1. Generation of detachment angle of aluminum flake in ECS

During the process of ECS for separating aluminum from plastic, repulsive force will be generated between aluminum and magnet as aluminum flake gets into the magnetic field of the separator. The direction of repulsive force has been given in Fig. 6, and the force will increase as the aluminum moves closer to the magnets of separator. The repulsive force can be divided into the vertical component and the horizontal component (see Fig. 6). Horizontal component is counteracted with the friction force (f) coming from the conveyor belt. Vertical component of the repulsive force is balanced out by the gravity force of the aluminum flake. When the aluminum flake arrives at the position of point (x_0, y_0) given in Fig. 6, due to the increasing of the repulsive force, the vertical component of repulsive force will be greater than the gravity force (G). Aluminum flake will have a vertical-upward acceleration and move upward. Thus, position of point (x_0, y_0) is considered as the detachment point of aluminum from separator surface in ECS. Angle α_0 plotted in Fig. 6 is defined as the detachment angle of aluminum flake from the conveyor belt in ECS.

2.3.2. The calculation of the detachment angle

Repulsive force between aluminum flake and inducing magnet causes the flake levitated. Seen from the simulation imagination of the density distribution of the magnetic field (Fig. 4), the strong magnetic density mainly distributes in the surface of separator. Magnetic flux of the separator can be assumed as crossing over the flake vertically when levitation happens. Thus, horizontal component of the repulsive force can be neglected and:

$$Fr \approx F_\perp$$

$F_\perp$ is vertical component of the repulsive force. When $F_\perp$ is greater than the gravity force (G), aluminum flake will detach from the conveyor belt.

$$F_\perp \geq G \quad (13)$$

The curves of the repulsive forces of aluminum flakes (C1, C2, R1, R2, T1, and T2) in ECS were plotted under the operation parameters of feeding speed 0.4 m/s, rotation speed of magnetic field 400 rpm and 800 rpm of the eddy current separator. The results are given in Fig. 7. Meanwhile, the curves of the gravity forces of various aluminum flakes were also plotted and given in Fig. 7. The intersection point of the curves of repulsive force and gravity force is the detachment angle of aluminum flake from the conveyor belt. It can be seen from Fig. 6 that range of the angle (α_0) was from 0° to 90°. Thus, values of intersection points of the two curves were calculated in this range. The detachment angles (α_0) of the aluminum flakes (C1, C2, R1, R2, T1, and T2) in ECS are presented in Fig. 7. The range of detachment angles of the aluminum flakes is from 7.5° to 14.9°.

2.4. Results of testing experience of detachment angle

In order to test the calculation results of detachment angles, experiment of ECS was performed in lab. The selected aluminum flakes (C1, C2, R1, R2, T1, and T2) were fed into ECS. Digital camera was used to catch the detachment angles of aluminum flakes. The detachment moment of the flake from conveyor belt was very short and it was difficult to be caught by camera timely. Thus, the separation process was repeated several times in order to catch the most accurate detachment angle. Many photos that presented the detachment moment of aluminum flake enough clearly were gained in the experiment. Every detachment angle in these photos was measured by protractor. The photos that presented the minimal and maximum detachment angles of aluminum flakes from the conveyor belt of separator were picked out and presented in Fig. 8. It indicated that the range of the detachment angles of aluminum flakes (C1, C2, R1, R2, T1, and T2) in testing experiment was from 8° to 15°. This range was approximately agreed with the calculation result.

2.5. Calculation of the detachment angle of aluminum flake (C2) by other model

In order to show the different between the new model and the other model, we calculated the detachment angle of aluminum flake C2 by the other model [16]. The reason of choosing C2 is that it had the minimal detachment angle in the calculation of detachment angle of the flakes (C1, C2, R1, R2, T1, and T2). The parameters of ECS were supposed as feeding speed 0.4 m/s and rotation speed of magnetic field 400 rpm in the calculation. Detachment angle of aluminum flake C2 calculated by the other model was 6.9°. It is different from the result (7.5°) calculated by the new model. Compared to the results of the minimal detachment angles (8°) in testing experiment, detachment angle (7.5°) calculated by the new model is more approach to the experiment data.

3. Conclusion

Based on the conception of supposing the nonferrous particle as an induced magnetic pole in ECS, a new model of the repulsive force that generated between aluminum flake and separator magnet was constructed in this paper. The purpose of constructing the model is to investigate the impact factors of the ECS process of waste TCs recovering. Compared to the literatures of the repulsive force, the model added some unreported impact factors of ECS such as S_m (area of per magnet that facing the particle) and S_p (maximal cross area of the flake in horizontal). Furthermore, the orientation factors (δ) of circle, rectangle, and triangle aluminum flakes in ECS were detailed expressed. Detachment angles of aluminum flakes from the conveyor belt were calculated based on the model of repulsive force. The calculation results were agreed with the results of testing experiment. Therefore, the new model of repulsive force is suitable to guide the ECS process of waste TCs recovering.

References

[1] J. Li, H. Lu, J. Guo, Z. Xu, Y. Zhou, Recycle technology for recovering resources and products from waste printed circuit boards, Environ. Sci. Technol. 41 (2007) 1995–2000.
[2] J. Li, Z. Xu, Environmental friendly automatic line for recovering metal from waste printed circuit boards, Environ. Sci. Technol. 44 (2010) 1418–1423.
[3] J. Cui, E. Forssberg, Mechanical recycling of waste electric and electronic equipment: a review, J. Hazard. Mater. 99 (2003) 243–263.
[4] H.M. Veit, A.M. Bernardes, Recovery of copper from printed circuit boards scraps by mechanical processing and electrometallurgy, J. Hazard. Mater. 137 (2006) 1704–1709.
[5] Y. Park, D. Fray, Recovery of high purity precious metals from printed circuit boards, J. Hazard. Mater. 164 (2009) 1152–1158.
[6] K. Huang, J. Guo, Z. Xu, Recycling of waste printed circuit boards: a review of current technologies and treatment status in China, J. Hazard. Mater. 164 (2009) 399–408.
[7] J. Ruan, J. Li, Z. Xu, An environmental friendly recovery production line of waste toner cartridges, J. Hazard. Mater. 185 (2010) 696–702.
[8] M. Lungu, Z. Schlett, Vertical drum eddy-current separator with permanent magnets, Int. J. Miner. Process. 63 (2001) 207–216.
[9] A. Gesing, Assuring the continued recycling of light metals in end-of-life vehicles: a global perspective, JOM 56 (2004) 18–27.
[10] P. Puri, P. Compston, V. Pantano, life cycle assessment of Australian automotive door skins, Int. J. Life Cycle Assess. 14 (2009) 420–428.
[11] S. Zhang, E. Forssberg, J. Houwelingen, P. Rem, L. Wei, End-of-life electric and electronic equipment management towards the 21st century, Waste Manage. Res. 18 (2000) 73–85.
[12] S. Zhang, E. Forssberg, B. Arvidson, W. Moss, Aluminum recovery from electronic scrap by High-Force eddy-current separator, Resour. Conserv. Recycl. 37 (2002) 55–60.
[13] S. Zhang, E. Forssberg, Separation mechanisms and criteria of a rotating eddy-current separator operation, Resour. Conserv. Recycl. 25 (1999) 215–232.
[14] P. Rem, P. Leest, A. van den Akker, A model for eddy current separation, Int. J. Miner. Process. 49 (1997) 193–200.
[15] F. Maraspin, P. Bevilacqua, P. Rem, Modeling the throw of metals and nonmetals in eddy current separations, Int. J. Miner. Process. 73 (2004) 1–11.
[16] S. Zhang, P. Rem, E. Forssberg, Particle trajectory simulation of two-drum eddy current separators, Resour. Conserv. Recycl. 26 (1999) 71–90.
[17] R. Meier-Staude, Z. Schlett, M. Lungu, A new possibility in eddy-current separation, Miner. Eng. 15 (2002) 287–291.
[18] M. Yan, X. Peng, Magnetic Base and Magnetic Materials, Zhejiang University press, Zhejiang, 2006 (in Chinese).